https://dx.doi.org/10.21577/0103-5053.20230041

J. Braz. Chem. Soc., Vol. 34, No. 9, 1303-1308, 2023

Article

Theoretical Study of 2,6-Dichloro-3-methyl-1,4-benzoquinone Interacting with Graphene

Leandro C. Sobrinho[a] *and Silvete Guerini*[a] *,[a]

[a]*Departamento de Física, Universidade Federal do Maranhão, 65080-805 São Luís-MA, Brazil*

Humans, animals and wildlife can suffer consequences due to exposure to toxic substances present in the environment, such as disinfection by-products, the halo benzoquinones, which are formed through reactions between chlorine and natural organic matter present in the water. In this paper, the interaction of 2,6-dichloro-3-methyl-1,4-benzoquinone with graphene layer was investigated by *ab initio* methods based on the density functional theory. The results show that 2,6-dichloro-3-methyl-1,4-benzoquinone adsorption changes the electronic properties of the nanostructure depending on molecule adsorption site. The calculated binding energies show that this molecule interacts with graphene through a chemical adsorption process when the 2,6-dichloro-3-methyl-1,4-benzoquinone molecule is parallel to the graphene layer. Our results are promising because they indicate the ability of graphene to serve as a filter for toxic substances present in the water.

Keywords: graphene, 2,6-dichloro-3-methyl-1,4-benzoquinone, DFT, electronic properties

Introduction

Water is a very important natural resource, and today, there is a great concern on the part of governments and the population in general to preserve and conserve it. Nowadays, due to its importance for the preservation of animal and plant life, there is a great need to treat wastewater using efficient and low-cost techniques in order to reuse it for general consumption in the future. Households and industries discard water with large amounts of inorganic and organic toxic substances, which are a great threat to the environment.

Halobenzoquinones (HBQs) are a class of chlorination disinfection by-products, which are mainly present in drinking water treatment plant effluents that may be relevant to bladder cancer risk.[1] The 2,6-dichloro-3-methyl-1,4-benzoquinone (DCMBQ) is mainly found in chlorinated drinking water.[2] Previous studies have shown that HBQs are highly cytotoxic,[3] as they can induce the generation of reactive oxygen species (ROS), deplete cellular glutathione (GSH)[4] and damage deoxyribonucleic acid (DNA) and proteins in mammalian cell lines.[5] Although much toxicological research has focused on understanding the toxicodynamics of HBQs, little attention has been paid to the removal of HBQs from the environment.

On the other hand, graphene has attracted a lot of attention due to its unique electrical, mechanical and thermal properties with applications in nanoelectronics, flexible electronics, sensors and solar cells.[6,7] The interactions of graphene with other compounds can lead to new properties, such as high conductivity and good stability in composite materials.[6] Several studies show that graphene is a good adsorbent for water pollutants[8,9] as well as for organic compounds. In addition, the graphene can also be used to remove algal toxins from water,[10] functionalized graphene oxide is good for removing Methylene Blue from real wastewater, while reduced graphene oxide is an efficient adsorbent to remove nitroaromatic compounds from water.[11,12]

The study of the adsorption of organic and inorganic compounds on graphene can highlight the use of this nanomaterial as an adsorbent to control environmental pollution. Graphene has become a good device for adsorbing pollutant molecules due to the changes in its electrical conductivity since these adsorbed molecules can act as acceptors or donors of electrons.[13,14]

In the literature there are several experimental works[7,9] that prove the efficiency of using graphene as an adsorbent to treat wastewater due to its very high surface area, excellent chemical stability and large delocalized π-electron systems. Thus, in this work, the structural, energetic and electronic properties of a single graphene layer interacting

*e-mail: silvete@gmail.com
Editor handled this article: Paula Homem-de-Mello (Associate)

with DCMBQ molecule were investigated through first-principles calculations based on density functional theory (DFT). Our calculations predict that the DCMBQ molecule can interact with the graphene layer through a physical or chemical process, depending on the adsorption site.

Methodology

The investigation of DCMBQ adsorption in different sites of the graphene layer was made through first-principles density functional theory (DFT) calculations.[15] The SIESTA software[16] was used to solve the Kohn-Sham equations through fully self-consistent calculations.[17] The interaction between the valence electrons and ionic cores was described through norm-conserving pseudopotentials[18] in the Kleinman-Bylander form.[19] In all the calculations, a double zeta basis set with polarization function (DZP) was used.[20] A 5 × 5 × 5 Monkhorst-Pack method[21] was used to sample the Brillouin zone. To make sure that we correctly described the interaction of the DCMBQ molecule with the graphene layer, we compared two different exchange-correlation functionals: the local density approximation (LDA) with the Ceperley and Alder parameterization[22] and the other with the van der Waals correction (vdW-DF/DRSLL),[23,24] which tries to include London dispersion interactions in the DFT. The charge density was represented by a cutoff of 150 Ry for the grid integration.

The supercell approximation and the periodic boundary conditions were used in all calculations. The graphene layer supercell was constructed with 128 atoms in a hexagonal lattice. The structural optimizations were performed through a conjugated gradient procedure and the atomic positions were relaxed until all the force components were smaller than 0.05 eV $Å^{-1}$.

The calculated binding energies (E_b) using the LDA and vdW-DF/DRSLL functionals were obtained through equation 1:

$$E_b = E_T(GR + DCMBQ) - E_T(GR) - E_T(DCMBQ) \quad (1)$$

where E_T(GR + DCMBQ) represents the total energy of the graphene layer with the DCMBQ molecule adsorbed on its surface in different sites, E_T(GR) corresponds to the total energy of the pristine graphene layer and E_T(DCMBQ) the total energy of the isolated DCMBQ molecule. Since SIESTA uses pseudo-atomic orbitals to describe the Kohn-Sham orbitals, the dimensions of the basis sets are different for each term of equation 1, that is, as the E_T(DCMBQ + GR) represents the total energy of graphene with the adsorbed molecule, so it is described by a complete basis set since it includes both the basis set of the molecule and the graphene layer. Thus, the E_T(DCMBQ) and E_T(GR + DCMBQ) terms are described through an incomplete basis set compared to the E_T(GR + DCMBQ) term, as they do not include the basis set of the molecule and the graphene layer together. Therefore, the basis set superposition error (BSSE)[25] was calculated for each system and included in the binding energy expression. This correction uses "ghost" atoms through the counterpoise method, as the equation 2 shows:

$$E_b^{BSSE} = E_T(GR + DCMBQ) - E_T(DCMBQ_{ghost} + GR) - E_T(DCMBQ + GR_{ghost}) \quad (2)$$

where, the subscript "ghost" corresponds to additional basis set functions centered at the position of the DCMBQ molecule or graphene layer, but without any atomic potential.

Results and Discussion

In our study, we investigated the interaction of the DCMBQ molecule with the graphene layer at different positions. The optimized geometries to six configurations more stable are shown in Figures 1a-1f. The studied configurations are:

(*i*) DCMBQ molecule parallel to the graphene layer with one graphene carbon atom on the center of the aromatic ring of the molecule (Figure 1a);

(*ii*) DCMBQ molecule parallel to graphene layer with the aromatic ring of the molecule parallel to one aromatic ring of graphene (Figure 1b);

(*iii*) DCMBQ molecule perpendicular to the graphene layer with two chlorine and one oxygen towards the graphene layer (Figure 1c);

(*iv*) DCMBQ molecule perpendicular to the graphene layer with one chlorine, one hydrogen and one oxygen towards the graphene layer (Figure 1d);

(*v*) DCMBQ molecule perpendicular to the graphene layer with two hydrogens and one oxygen towards the graphene layer (Figure 1e);

(*vi*) DCMBQ molecule perpendicular to the graphene layer with the methyl group towards the graphene layer (Figure 1f).

The configuration shown in Figure 1a was predicted to be the most stable, in which the C–O, C–Cl and C–C bond distances are approximately 2.81, 3.24 and 3.04 Å, respectively, while in the configuration shown in Figure 1b, these same bonding distances (C–O, C–Cl and C–C) are around 2.85, 3.28 and 3.11 Å, respectively. Table 1 lists the shortest distances between the DCMBQ molecule and the graphene layer in all configurations shown in Figure 1.

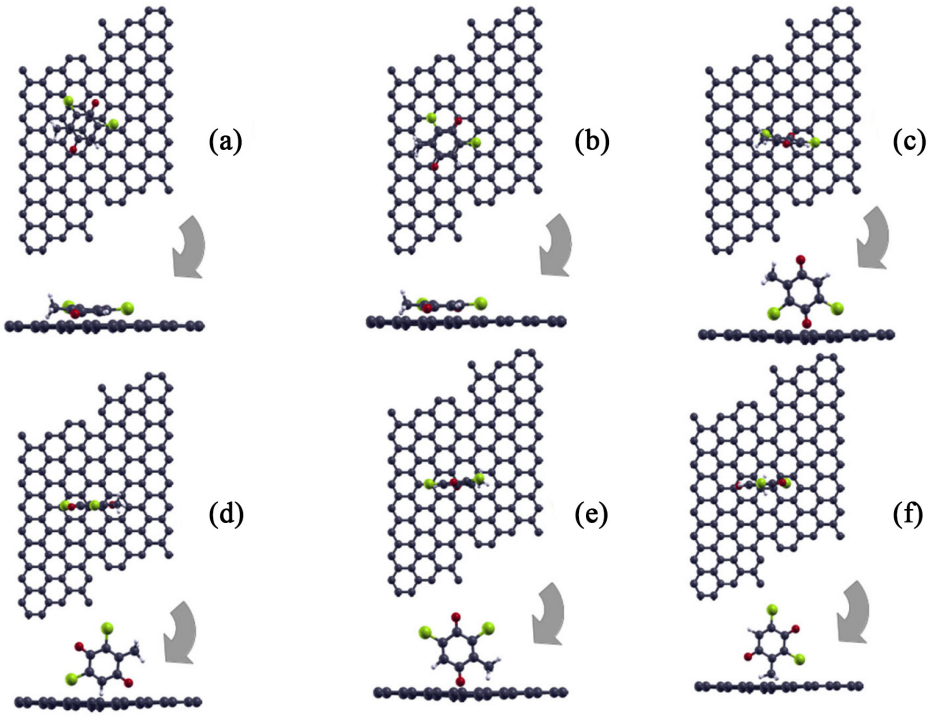

Figure 1. Top and side views of the optimized structures for interaction of the graphene with the DCMBQ molecule in different positions. The black, red, green and white spheres represent C, O, Cl and H atoms, respectively. (a) Configuration *i*, (b) configuration *ii*, (c) configuration *iii*, (d) configuration *iv*, (e) configuration *v*, (f) configuration *vi*.

Table 1. The shortest distances (D) between the molecule and graphene and charge transfer (CT) calculated for all configurations shown in Figure 1. The plus sign in the charge transfer values indicates that the DCMBQ molecule receive electronic charge

System	D / Å	CT / e$^-$
i	C–O = 2.81	+0.18
ii	C–O = 2.85	+0.20
iii	C–H = 2.17	+0.18
iv	C–O = 2.61	+0.11
v	C–H = 2.68	+0.14
vi	C–Cl = 2.88	+0.10

The Mülliken population[26] analysis was performed in all studied configurations and used to predict the electronic charge transfer (shown in Table 1) between the graphene and the DCMBQ molecule, in which we verify that DCMBQ molecule behaves as an electron acceptor in all cases. In configuration (*i*), which is the most stable, the DCMBQ received 0.18 e$^-$, while in configurations (*ii*) and (*iii*), it received 0.20 and 0.18 e$^-$, respectively. The charge transfer in these cases occurs through a chemical or physical process, according to the binding energy values (see Table 2).

Table 2 shows the binding energies obtained using the LDA and vdW-DF/DRSLL functional. Comparing the binding energy values obtained in both functional, we verify that there is no difference in the stability trend, but the binding energy values increased in absolute value when the vdW functional was used. Although the BSSE correction did not change the stability trend, however, it greatly decreased the values of the binding energies in absolute value, which also decreased the stability of each system.

Table 2. Binding energies calculated for each configuration shown in Figure 1, using the LDA (E_b^{lda}) and vdW-DF/DRSLL (E_b^{vdw}) functionals. The E_b^{bsse} corresponds to the E_b^{lda} with BSSE correction

System	Binding energy / eV		
	E_b^{lda}	E_b^{vdw}	E_b^{bsse}
i	–0.99	–1.87	–0.60
ii	–0.89	–1.86	–0.48
iii	–0.42	–1.11	–0.20
iv	–0.38	–0.92	–0.12
v	–0.28	–0.57	–0.10
vi	–0.23	–0.89	–0.09

All results from here on were performed only with the LDA functional. Although the LDA overestimates the binding energy, it provides reliable results for electronic properties. Therefore, the binding energy analysis of the studied configurations (see Figure 1) shows that the interaction between DCMBQ molecule and the graphene layer can be either a physical or chemical adsorption process,

depending on the adsorption site. The binding energy values also show that the configurations with the DCMBQ molecule parallel to the graphene layer (Figures 1a and 1b) are the most favorable energetically, which have binding energies around –0.99 and –0.89 eV, respectively. These values also show that the adsorption between the DCMBQ molecule and the graphene layer is substantially dependent on the interaction between the DCMBQ's aromatic ring and the graphene's aromatic rings, so we infer that the energetic stability of the adsorbed DMCBQ molecule is ruled by the π-staking interactions between the electrons of the DMCBQ molecule and graphene layer. Following the analysis carried out by Castro *et al.*,[27] we suggest that the adsorption of this molecule on the graphene surface occurs via a chemical process, in configurations (*i*) and (*ii*) of Figure 1. While in all the other configurations (Figures 1c-1f), the adsorption occurs through a physical process.

To analyze the modification in the electronic properties of the graphene layer interacting with the DCMBQ molecule, the band structure near the Fermi level was plotted in Figure 2, for each configuration of the Figure 1 and for the pristine graphene layer. The latter was plotted for comparison purposes, in Figure 2a. Figures 2b-2g correspond to the band structures of the configurations (*i*)-(*vi*) of Figure 1, respectively. We observed changes in each band structure when the DCMBQ molecule interacts with the graphene layer (Figures 2b-2g), mainly in the valence and conduction bands, however, these changes strongly depend on the molecule's adsorption site. The first change is that all systems are metallic, as shown by the band structures plotted in Figures 2b-2g, where the energy levels introduced by the DCMBQ molecule are dispersed in both valence and conduction bands.

Figures 2b and 2c represent the band structures of the two most stable configurations (*i* and *ii*, respectively), where we can see that the adsorption of the DCMBQ molecule separates the energy levels in the Dirac cone and introduces a partially delocalized energy level along the M-K direction. We plotted the charge density to better elucidate the localization of these energy levels in the region between –4.83 to –4.52 eV. The plot indicates that these levels are contributions from the carbon and oxygen atoms of the DCMBQ molecule, as shown in Figures 3a and 3b, respectively. Furthermore, in both band structures (Figures 2b and 2c), new degenerate levels appear in valence and conduction bands, and the Fermi level is shifted by 0.19 eV to the valence band when compared to the pristine graphene band structure (Figure 2a). In Figures 2d-2g, which the band structures of the configurations (*iii*)-(*vi*) were plotted respectively, new energy levels have appeared mainly in the conduction band. In Figure 2d, the Fermi level is shifted by 0.10 eV to the valence band, one localized level appears at approximately 0.25 eV above the Fermi level. The plot of charge density around the Fermi level, –4.98 to –4.60 eV region, shows that these contributions are from the carbon and oxygen atoms of the molecule (see Figure 3c). For the band structures shown in Figures 2e-2g, we observed that the Fermi level was also shifted by 0.14, 0.08 and 0.14 eV,

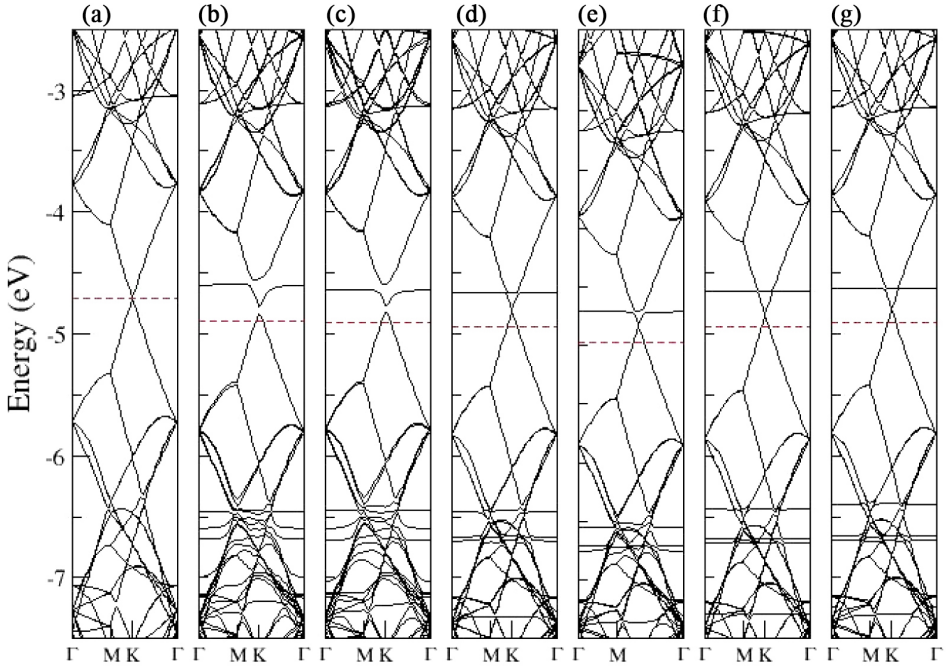

Figure 2. Electronic band structures for (a) (P) the pristine graphene layer and for (b-g) (*i*)-(*vi*) different configurations of the DCMBQ adsorbed on graphene layer, which correspond to the configurations shown in Figures 1a-1f, respectively. The dotted horizontal red line corresponds to the Fermi level.

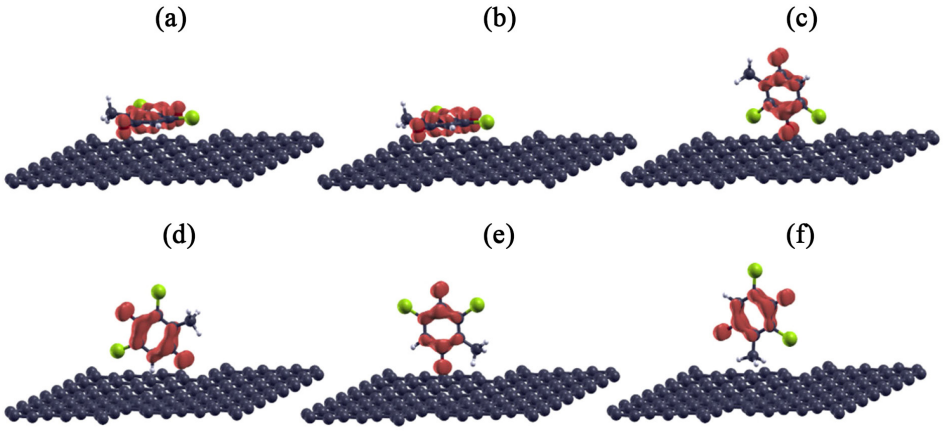

Figure 3. Charge density contour plot for the DCMBQ molecule interacting with the graphene layer, in all studied configurations. The plots are for the band structures of the Figures 2b-2g, respectively, in the following regions: (a) configuration *i*, –4.83 to –4.52 eV, (b) configuration *ii*, –4.83 to –4.52 eV, (c) configuration *iii*, –4.88 to –4.58 eV, (d) configuration *iv*, –4.77 to –4.60 eV, (e) configuration *v*, –4.77 to –4.53 eV, (f) configuration *vi*, –4.78 to –4.60 eV. The isovalue used was 0.005 e Å^{-3} for all isosurfaces.

respectively, to the valence band, and new localized levels appeared above the Fermi level. The charge density plots for these levels show that they are contributed exclusively by the DCMBQ atoms, as shown in Figures 3d-3f. And, in all band structures, we infer that the shift of the Fermi level towards the valence band is associated with a charge transfer from graphene to DCMBQ molecule.

Currently, many aquatic systems are contaminated with different inorganic and organic toxic substances from wastewater of various anthropogenic sources, such as industries, agriculture, mining and homes. So, effluent treatment is an environmental challenge; however, this work shows that graphene is a good adsorbent for DCMBQ molecule. Therefore, we suggest that graphene can be used as a filter for toxic substances in the aquatic environment.

On the other hand, previous analyses[27-29] considering an approach similar to the procedure presented in this study, with other contaminants adsorbed on other nanomaterials, demonstrated that, generally, there is physical adsorption of molecules on the surfaces of nanomaterials, which is important to provide the desorption of these contaminants, and in this way, the nanostructures can be reused.

Conclusions

In summary, the electronic properties of the DCMBQ molecule interacting with graphene layer were investigated through first-principles calculations. It was observed that the electronic properties and the charge transfer process are sensitive to the DCMBQ adsorption site. The configurations where the DCMBQ molecule is parallel to the graphene layer are predicted to be the most stable systems due to π-π interactions between the aromatic rings from both the DCMBQ molecule and the graphene layer. Depending on the adsorption site, the DCMBQ molecule interacts with the graphene layer through a chemical or physical process. According to our results, we infer that graphene is a very promising material for DCMBQ adsorption and can be used as a polluted water filter since there are no chemical bonds between graphene and DCMBQ. The absence of chemical bonds is one of the necessary conditions for using graphene as a possible filter for removing pollutants from water.

Acknowledgments

The authors acknowledge to Coordenação de Aperfeiçoamento de Pessoal de Nível Superior (CAPES) for financial support. We are also grateful to CENAPAD-SP and LSIM-UFMA for the computational resources.

References

1. Wang, W.; Qian, Y.; Jmaiff, L. K.; Hrasner, S. W.; Hrudey, S. E.; Li, X.-F.; *Environ. Sci. Technol.* **2015**, *49*, 9898. [Crossref]
2. Zhao, Y.; Qin, F.; Boyd, J. M.; Anichina, J.; Li, X.-F.; *Anal. Chem.* **2010**, *82*, 4599. [Crossref]
3. Du, H.; Li, J.; Moe, B.; McGuigan, C. F.; Shen, S.; Li, X.-F.; *Environ. Sci. Technol.* **2013**, *47*, 2823. [Crossref]
4. Li, J.; Wang, W.; Moe, B.; Wang, H.; Li, X.-F.; *Chem. Res. Toxicol.* **2015**, *28*, 306. [Crossref]
5. Li, J.; Wang, W.; Zhang, H.; Le, X. C.; Li, X.-F.; *Toxicol. Sci.* **2014**, *141*, 335. [Crossref]
6. Pumera, M.; *Electrochem. Commun.* **2013**, *36*, 14. [Crossref]
7. Ko, G.; Kim, H.-Y.; Ahn, J.; Park, J.-M.; Lee, K.-Y.; Kim, J.; *Curr. Appl. Phys.* **2010**, *10*, 1002. [Crossref]
8. Alia, I.; Basheer, A. A.; Mbianda, X. Y.; Burakov, A.; Galunin, E.; Burakova, I.; Mkrtchyan, E.; Tkachev, A.; Grachev, V.; *Environ. Int.* **2019**, *127*, 160. [Crossref]

9. Sarker, M.; Song, J. Y.; Jhung, S. H.; *Chem. Eng. J.* **2018**, *335*, 74. [Crossref]
10. Pavagadhi, S.; Tang, A. L. L.; Sathishkumar, M.; Loh, K. P.; Balasubramanian, R.; *Water Res.* **2013**, *47*, 4621. [Crossref]
11. Wu, Z.; Zhong, H.; Yuan, X.; Wang, H.; Wang, L.; Chen, X.; Zeng, G.; Wu, Y.; *Water Res.* **2014**, *67*, 330. [Crossref]
12. Chen, X.; Chen, B.; *Environ. Sci. Technol.* **2015**, *49*, 6181. [Crossref]
13. Schedin, F.; Geim, A. K.; Morozov, S. V.; Hill, E. W.; Blake, P.; Katsnelson, M. I.; Novoselov, K. S.; *Nature Mater.* **2007**, *6*, 652. [Crossref]
14. Moseley, P. T.; *Meas. Sci. Technol.* **1997**, *8*, 223. [Crossref]
15. Hohenberg, P.; Kohn, W.; *Phys. Rev.* **1964**, *136*, B864. [Crossref]
16. Ordejón, P.; Artacho, E.; Soler, J. M.; *Phys. Rev. B* **1996**, *53*, 10441. [Crossref]
17. Kohn, W.; Sham, L. J.; *Phys. Rev.* **1965**, *140*, A1133. [Crossref]
18. Troullier, N.; Martins, J. L.; *Phys. Rev. B* **1991**, *43*, 1993. [Crossref]
19. Kleinman, L.; Bylander, D. M.; *Phys. Rev. Lett.* **1982**, *48*, 1425. [Crossref]
20. Artacho, E.; Sáchez-Portal, D.; Ordejón, P.; Garcia, A.; Soler, J. M.; *Phys. Status Solidi B* **1999**, *215*, 809. [Crossref]
21. Monkhorst, H. J.; Pack, J. D.; *Phys. Rev. B* **1976**, *13*, 5188. [Crossref]
22. Ceperley, D. M.; Alder, B. J.; *Phys. Rev. Lett.* **1980**, *45*, 566. [Crossref]
23. Dion, M.; Rydberg, H.; Schröder, E.; Langreth, D. C.; Lundqvist, B. I. V.; *Phys. Rev. Lett.* **2004**, *92*, 246401. [Crossref]
24. Román-Pérez, G.; Soler, J. M.; *Phys. Rev. Lett.* **2009**, *103*, 096102. [Crossref]
25. Boys, S. F.; Bernardi, F.; *Mol. Phys.* **1970**, *19*, 553. [Crossref]
26. Mülliken, R. S.; *J. Chem. Phys.* **1955**, *23*, 1841. [Crossref]
27. Castro, S. M.; Ribeiro, H. C.; Araújo, A. B.; Guerini, S.; *J. Braz. Chem. Soc*. **2020**, *31*, 768. [Crossref]
28. Castro, S. M.; Araújo, A. B.; Nogueira, R. F. P.; Guerini, S.; *Appl. Surf. Sci.* **2017**, *403*, 519. [Crossref]
29. da Silva, A. A. J.; Caetano, C. V.; Guerini, S.; *J. Mol. Model.* **2021**, *27*, 234. [Crossref]

Submitted: December 29, 2022
Published online: March 23, 2023